OXFORD

Cerebral Cortex, 2022, **00**, 1–11
https://doi.org/10.1093/cercor/bhab493
Original Article

Concurrent TMS-EEG to Reveal the Neuroplastic Changes in the Prefrontal and Insular Cortices in the Analgesic Effects of DLPFC-rTMS

Yang Ye[1,2], Jinghua Wang[3,4] and Xianwei Che[1,2]

[1]Centre for Cognition and Brain Disorders, The Affiliated Hospital of Hangzhou Normal University, Hangzhou 310015, China
[2]Institute of Psychological Sciences, Hangzhou Normal University, Hangzhou 311121, China
[3]Department of General Practice, The Affiliated Hospital of Hangzhou Normal University, Hangzhou 310015, China
[4]Department of General Practice, Deqing Hospital of Hangzhou Normal University, Hangzhou 313201, China

Address correspondence to Dr Xianwei Che, Centre for Cognition and Brain Disorders, The Affiliated Hospital of Hangzhou Normal University, Building 27, 2318 Yuhangtang Road, Hangzhou 311121, China. Email: xwcheswu@gmail.com.

Abstract

The dorsolateral prefrontal cortex (DLPFC) is an important target for repetitive transcranial magnetic stimulation (rTMS) to reduce pain. However, the analgesic efficacy of DLPFC-rTMS needs to be optimized, in which the mechanisms of action remain unclear. Concurrent TMS and electroencephalogram (TMS-EEG) is able to evaluate neuroplastic changes beyond the motor cortex. Using TMS-EEG, this study was designed to investigate the local and distributed neuroplastic changes associated with DLPFC analgesia. Thirty-four healthy adults received DLPFC or sham stimulation in a randomized, crossover design. In each session, participants underwent cold pain and TMS-EEG assessment both before and after 10-Hz rTMS. We provide novel findings that DLPFC analgesia is associated with a smaller N120 amplitude in the contralateral prefrontal cortex as well as with a larger N120 peak in the ipsilateral insular cortex. Furthermore, there was a strong negative correlation between N120 changes of these two regions whereby the amplitude changes of this dyad were associated with increased pain threshold. In addition, DLPFC stimulation enhanced coherence between the prefrontal and somatosensory cortices oscillating in the gamma frequency. Overall, our data present novel evidence on local and distributed neuroplastic changes associated with DLPFC analgesia.

Keywords: DLPFC, pain, plasticity, TMS, TMS-EEG

Highlights

- Concurrent TMS-EEG was used to evaluate neuroplastic changes in DLPFC analgesia.
- DLPFC analgesia was associated with a smaller N120 peak in the prefrontal cortex.
- DLPFC analgesia was also related to a larger N120 peak in the insular cortex.
- There was a strong negative correlation between N120 changes of these two regions.
- DLPFC-rTMS enhanced the prefrontal and somatosensory coupling in the gamma frequency.

Introduction

Transcranial magnetic stimulation (TMS) is a safe and noninvasive form of brain stimulation. Repetitive TMS (rTMS) can induce neuroplastic changes, which has been used to manage chronic pain conditions such as neuropathic pain (Pascual-Leone et al. 1998; Passard et al. 2007; Lefaucheur et al. 2014). High-frequency (≥5 Hz) rTMS over the contralateral primary motor cortex (M1) can induce transient analgesic effects (Lefaucheur et al. 2014). In addition, the dorsolateral prefrontal cortex (DLPFC) has been increasingly used as an alternative target in pain management (Short et al. 2011; Leung et al. 2018; Hosomi et al. 2020) due to its capacity in the modulation of pain experience (Tracey and Mantyh 2007). Indeed, our group has recently demonstrated an analgesic effect of DLPFC-rTMS in neuropathic pain conditions (Che, Cash, et al. 2021).

However, DLPFC-rTMS may not be able to induce long-lasting analgesia as indicated by the current literature (Che, Cash, et al. 2021). Moreover, the mechanisms of action associated with DLPFC analgesia are still unclear. Understanding the mechanisms of DLPFC analgesia may therefore help to optimize the analgesic efficacy of DLPFC stimulation. There is evidence that excitatory stimulation of this region may evoke top-down modulation of descending pain systems in brainstem regions, such as the periaqueductal gray (PAG) and the rostral ventromedial medulla (RVM) (Martin et al. 2013; Taylor et al. 2013; De Martino et al. 2019). For instance, the analgesic effect of DLPFC-rTMS was found to be

Received: August 31, 2021. **Revised:** November 21, 2021. **Accepted:** December 1, 2021

associated with enhanced brain activity in the prefrontal cortex but with decreased activity in the midbrain and medulla regions (Taylor et al. 2013).

In addition to the top-down mechanisms, cortical excitability is a promising mechanism as repeated sessions of rTMS restored defective intracortical inhibition in chronic pain (Lefaucheur et al. 2006). Concurrent TMS and electroencephalogram (TMS-EEG) is able to evaluate neuroplastic effects of rTMS delivered over nonmotor regions, such as the prefrontal cortex (Fitzgerald et al. 2008; Cash et al. 2017). TMS-evoked potentials (TEPs) are believed to reflect the shifts in the inhibition–excitation balance in cortical circuits following a single TMS pulse (Premoli, Castellanos, et al. 2014; Du, Rowland, Summerfelt, Choa, et al. 2018; Du, Rowland, Summerfelt, Wijtenburg, et al. 2018), which have been demonstrated to be stable and reproducible cortical responses (Ozdemir, Boucher, et al. 2021; Ozdemir, Tadayon, et al. 2021). Among them, N120 has the highest signal-to-noise ratio (SNR), which is considered to reflect $GABA_B$-mediated intracortical inhibition (Premoli, Castellanos, et al. 2014; Premoli, Rivolta, et al. 2014; Darmani et al. 2019). Our group has previously demonstrated N120 changes in the prefrontal cortex following DLPFC-rTMS (Chung et al. 2017; Che et al. 2019).

In addition, concurrent TMS-EEG is also able to evaluate neuroplasticity changes in distributed regions by means of neural oscillations and network properties (Chung et al. 2017; Premoli et al. 2017; Pisoni et al. 2018). For instance, TMS-EEG revealed a frontoparietal pathway which seems to distinguish self and others' somatosensory states (Pisoni et al. 2018). As described above, DLPFC stimulation is capable of modulating descending pain systems (Taylor et al. 2013). Moreover, DLPFC is also believed to modulate corticocortical pathways involved in analgesia, such as the insular cortex and the anterior cingulate cortex (ACC) (Lorenz et al. 2003). Evaluating the neuroplastic changes in distributed regions may, therefore, refine the understanding of DLPFC analgesia associated with and potentially beyond top-down pain modulation.

Using TMS-EEG, the current study was designed to investigate the local and distributed neuroplastic changes associated with DLPFC analgesia. We hypothesized that the analgesic effect of DLPFC-rTMS would be associated with increased neural activity in the prefrontal cortex assessed with TEPs. We also explored the neuroplastic changes in prefrontal connections following DLPFC stimulation, with a focus on neuroplastic changes in corticocortical pathways involved in pain and analgesia.

Materials and Methods

Participants

An a priori sample size calculation (alpha = 0.05, beta = 0.8, Cohen's $d = 0.5$) indicated a minimum of 34 participants for the study to be sufficiently powered. A group of 36 healthy, right-handed, TMS-eligible (Rossi et al. 2011) adults were recruited to account for potential dropouts. Exclusion criteria included a history or current diagnosis of psychiatric disorder, or use of psychoactive medication, as assessed by the Mini International Neuropsychiatric Interview (MINI) (Sheehan and Lecrubier 2001). Two participants withdrew from this study after the first session. Data from 34 participants (age range: 18–25 years, mean ± SD: 20.85 ± 2.03, 20 female) were therefore analyzed. Among these participants, 85% (29/34) were naïve to any form of TMS, and five of them reported to have a most recent TMS experience at least two weeks ago. All participants provided a written informed consent prior to the experiment. This study was approved by the Ethics Committee in the Centre for Cognition and Brain Disorders of the Hangzhou Normal University (20201218) and was conducted in accordance with the Declaration of Helsinki.

Experimental Design and Procedure

This was a single-blind, crossover, and sham-controlled study. Participants visited the laboratory at two time points (≥72 h, Mean ± SD: 7.34 ± 6.05 days), receiving a single session of DLPFC or sham stimulation with the sequence being pseudorandomized and counterbalanced. Before and after rTMS, 105 single pulses were delivered to the DLPFC in order to assess neuroplastic changes. Participants also underwent a cold pain protocol before and after rTMS in each session.

Resting Motor Threshold and Single-Pulse TMS-EEG

Resting motor threshold (RMT), defined as the minimum intensity to induce motor-evoked potentials (MEPs) > 0.05 mV of the first dorsal interosseous (FDI) muscle in 5/10 trials, was measured before each session. Single pulses to the hand region of the left M1 (45° to the midline, handle pointing backward) at 5 s ± 10% jitter intervals were sent by a figure-eight coil connected to a Magstim Rapid^2 system (Magstim Company Ltd). It is noted that RMT was determined after the EEG setup for consistency as rTMS was delivered in the same setting. Coil position was measured relative to the nasion and inion to facilitate consistent repositioning of the coil between sessions (Rogasch et al. 2013; Chung, Rogasch, Hoy, and Fitzgerald 2018; Chung, Rogasch, Hoy, Sullivan, et al. 2018; Che, Fitzgibbon, et al. 2021).

Single pulses ($n = 105$) were delivered to the left DLPFC, which was located according to the Beam F3 algorithm (Beam et al. 2009). The coil was positioned at 90° relative to midline (handle pointing left, see Fig. 1*a*), with the intensity being set to 110% RMT (Che et al. 2019). A masking noise was played through earplugs during TMS-EEG recordings (Rocchi et al. 2018, 2021). The sound level was gradually increased until the participants reported to barely hear single-pulse TMS clicks at 110% RMT.

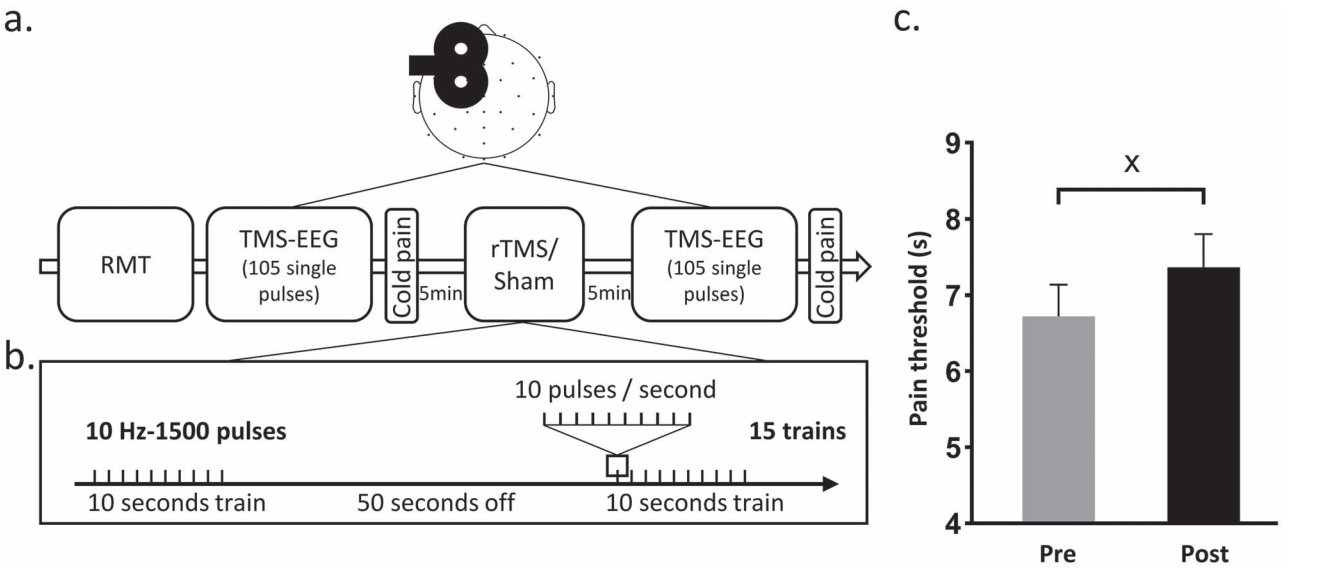

Figure 1. Study protocol and results. (*a*) Study protocol. (*b*) rTMS protocol. (*c*) Main effect of increased cold pain threshold ($P_{Bonf} = 0.037$) from pre- to poststimulation. X denotes $P < 0.05$. RMT denotes resting motor threshold.

EEG Recordings

EEG recordings during single-pulse TMS took place in a temperature-controlled, sound-attenuated, and electrically shielded room. Participants were seated in a chair with their eyes opening and looking forward. EEG data were recorded using 32 active electrodes mounted on a cap (Brain Products GmbH) according to the international 10–20 system, including Fp1, Fp2, F3, F4, C3, C4, P3, P4, O1, O2, F7, F8, T7, T8, P7, P8, Fz, Cz, Pz, FC1, FC2, CP1, CP2, FC5, FC6, CP5, CP6, TP9, TP10, CPZ, POz, Oz. FCz and AFz were specified as the reference and ground electrode, respectively. EEG impedances were kept below 10 kΩ throughout the recordings. It is noted that the cold pain equipment was turned off during EEG recordings to avoid noises.

Pain Protocol

A cold pain protocol has been repeatedly used in rTMS studies (Summers et al. 2004; Lefaucheur et al. 2008; Che, Fitzgibbon, et al. 2021). In this study, participants were asked to insert their right hand into a bucket of circulating cold water at 5 ± 0.1 °C (dhc-0505-a, http://www.qiweiyiqi.com/) (Rainville et al. 1992; Mitchell et al. 2004; Che, Fitzgibbon, et al. 2021). It is noted that the anticipation of pain could modulate pain experience (Wager et al. 2004; Vase et al. 2005). Participants were initially asked to insert their left hand into the cold water before pain assessment. During the exposure of left hand, participants were asked to describe their feelings of the cold water, with the purpose to experience the cold pain used here. Participants then dried their left hand and took a break before the cold pain assessment with the right hand.

Pain threshold was recorded as the time (in seconds) at which participants first reported cold pain (Lowery et al. 2003; Santarcangelo et al. 2013). As pain can affect corticospinal excitability, participants then took a break for 5 min during which they inserted the right hand into a hand warmer (~40 °C) to recover from the cold pain (Che, Fitzgibbon, et al. 2021).

Repetitive Transcranial Magnetic Stimulation

Repetitive TMS was delivered to the left DLPFC with an intensity of 80% RMT (Nahmias et al. 2009; de Andrade et al. 2014). The rTMS protocol included 15 trains of 10-s stimulation given at 10 Hz, with the intertrain interval being set to 50 s (1500 pulses) (Nahmias et al. 2009; de Andrade et al. 2011). The Sham stimulation was delivered using the same protocol, with the coil being orientated at 90° to the scalp so that the magnetic field would be delivered away from the scalp (Pascual-Leone et al. 1998).

TMS-EEG Data Analysis

TMS-EEG data were preprocessed as previously described (Chung et al. 2017; Che et al. 2019). Offline TMS-EEG data analysis was performed with EEGLAB (Delorme and Makeig 2004; Rocchi et al. 2021), FieldTrip (Oostenveld et al. 2011), and custom scripts running on Matlab (R2017a, The MathWorks, USA).

TMS-EEG signals were epoched around the TMS pulses (−1 to 2 s) and baseline corrected (−500 to −50 ms). The large magnetic pulses were then removed and interpolated (−5 to 20 ms). Although the time window (−5 to 20 ms) was slightly larger than that in the literature (−5 to 15 ms), TMS pulses were nicely removed and interpolated, leaving no clear decay artifacts in the following cleaning procedures (see Supplementary Materials). The epoched data were concatenated across the two time points (pre- and poststimulation) to avoid bias in component rejection. Data were then downsampled to 1000 Hz. Prior to independent component analysis (ICA), the epochs were visually inspected and those with excessive noise and/or disconnected electrodes were removed. Two rounds of FastICA were performed using

a semiautomated component classification algorithm (Rogasch et al. 2014, 2017). The first round of ICA was performed to remove large TMS-evoked muscle artifacts and decay artifacts (Rogasch et al. 2014). Data were then band-pass (1–100 Hz) and band-stop filtered (48–52 Hz) and epochs were visually inspected again to remove any anomalous activity. The second round of ICA was performed to remove residual artifacts (e.g., eyeblinks, continuous muscle activity, saccadic movement, electrode noises, etc.). Removed channels were then interpolated. Finally, EEG signals were re-referenced to the common average reference and split into original time points (Pre- and poststimulation). The final pulse numbers were (Mean ± SD): Pre_DLPFC: 95.94 ± 4.20; Pre_Sham: 96.24 ± 5.25; Post_DLPFC: 95.53 ± 5.99; and Post_Sham: 95.76 ± 8.06.

Source localization was further performed on TEP changes. The standardized low-resolution electromagnetic tomography algorithm (sLORETA) is able to calculate the three-dimensional distribution of neuronal activity in the cerebral cortex based on the scalp potential distribution (Pascual-Marqui 2002). This algorithm has been frequently used to estimate possible generators of neuronal oscillations or evoked potentials, with the results being validated using combined EEG-positron emission tomography (PET) and EEG-functional magnetic resonance imaging (fMRI) data (Pizzagalli et al. 2003; Mulert et al. 2004). In the current study, the current source density was primarily estimated in the 120 ms time window (90–130 ms) in which different amplitudes were observed form pre- to poststimulation.

Connectivity analysis was further performed on the TMS-EEG data by computing the debiased weighted phase lag index (WPLI) between channels. The WPLI is a measure of phase coherence of two signals, based on the imaginary part of the cross-spectrum (Pisoni et al. 2018). By doing so, WPLI allows to reduce the sensitivity of the index to additional, unrelated noise sources, such as volume conduction, as well as to increase statistical power to detect changes in phase synchronization (Vinck et al. 2011). In order to calculate the WPLI, TMS-EEG data were initially decomposed to time–frequency domains using the "mtmconvol" methodology, for example, delta (0–3 Hz), theta (4–7 Hz), alpha (8–12 Hz), beta (13–30 Hz), and gamma (31–100 Hz). Finally, the debiased WPLI was computed for each electrode pair, obtaining a 32×32 WPLI matrix for pre- and post-rTMS for each stimulation condition.

Statistical Analyses

Statistical analyses were performed in SPSS (version 22; IBM Corp). In cases the data did not meet the requirement for normality (Shapiro–Wilk test), data were winsorized by setting extreme values to the corresponding adjacent 5th or 95th percentile value (Wilcox 2011) (in total two participants). A repeated measures two-way analysis of variances (ANOVA) was performed to analyze the effects of stimulation (DLPFC or sham) and time (pre and post) as well as their interaction on the pain threshold.

For TEPs, statistical analyses were conducted using cluster-based permutation statistics at a global scalp level (Maris and Oostenveld 2007). The cluster-based permutation test provides a straightforward way to solve the problem of multiple comparisons across space (EEG channels) and time (Maris and Oostenveld 2007). This was done in Fieldtrip, an open-source MATLAB toolbox (Oostenveld et al. 2011). Statistics were performed on peaks of interest (N45: 30–50 ms, P60: 50–70 ms, N120: 90–130 ms and P200: 160–240 ms), which are the most common peaks described in the literature (Rogasch et al. 2014; Belardinelli et al. 2021) as well as illustrated by our data (Fig. 2). Paired *t*-tests were conducted across time points (post vs. pre) for each TMS condition. An observed statistics value was considered in the cluster permutation if it was below the threshold of 0.05 in at least two of the neighboring channels (Oostenveld et al. 2011). We performed 5000 iterations of trial randomization for generating the permutation distribution, controlling for multiple comparisons across space. A corrected *P*-value below 0.025 (two-tailed) was considered significant. Bivariate correlations were further computed to assess the relationship between TEP changes and changes in the pain threshold.

For sLORETA, statistical differences between time points (pre and post) were calculated as images of voxel-by-voxel *t* values. The localization of different cortical activities was based on the standardized electrical current density and resulted in 3D *t* score images (Pascual-Marqui 2002). In these images, cortical voxels of significant difference were identified using a nonparametric approach corrected at 0.05 determined by 5000 randomizations (Pascual-Marqui 2002; Che et al. 2018).

Connectivity WPLI values were statistically tested using the network-based statistic (NBS) toolbox (Zalesky et al. 2010). The NBS is a nonparametric statistical method which uses cluster analysis to perform null hypothesis testing across networks of values from pairs of potentially connected nodes (Zalesky et al. 2010). Paired *t*-tests were performed to examine significant connectivity from pre- to poststimulation for each condition (DLPFC and sham). A primary threshold for electrode pairs was set at $P < 0.005$ to ensure that only robust differences in connectivity between electrode pairs would be compared at the cluster level (Bailey et al. 2018). The secondary threshold for family-wise corrected cluster null hypothesis testing was $P < 0.025$ (two-tailed) (Che et al. 2019). Results were visualized using BrainNet viewer (Xia et al. 2013). It is noted that the NBS was primarily performed on the N120 time window, which showed significant TEP changes following stimulation (see below in Plastic Effects of rTMS on TEPs), with secondary analyses being performed on other time windows of interest.

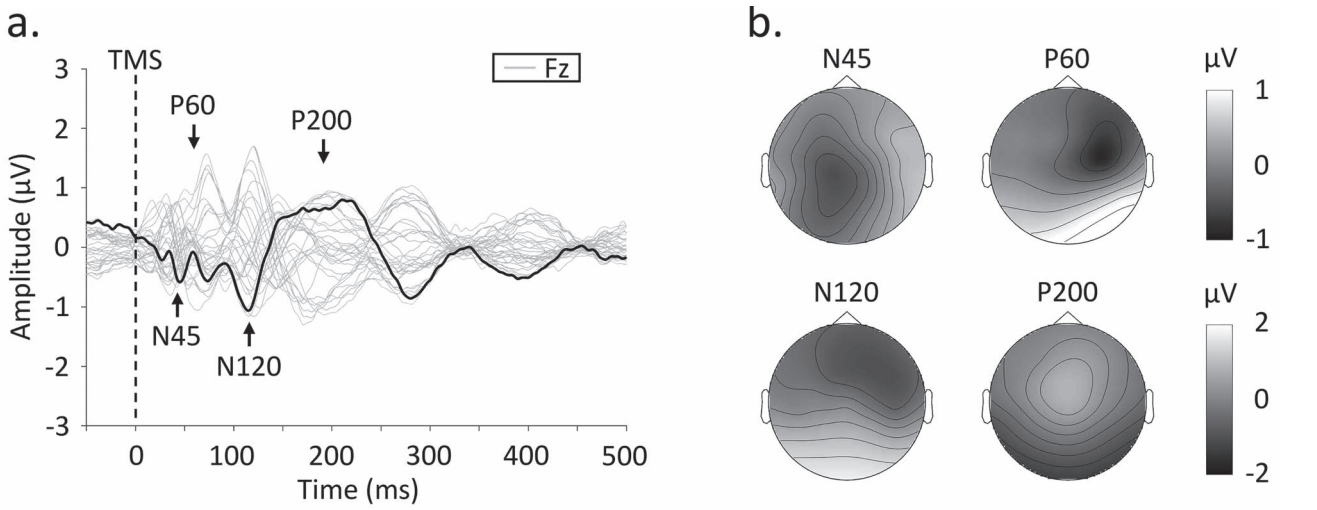

Figure 2. TEPs and voltage distribution following single-pulse TMS before the application of rTMS. Data were combined across the DLPFC- and sham-stimulation at baseline. (*a*) Butterfly plots of all electrodes with peaks of interest highlighted. The waveform in black line indicates the frontocentral electrode Fz for illustration purposes. (*b*) Topographical voltage distribution for the peaks of interest.

Supplementary Analysis

Supplementary analysis was performed on side effects of rTMS, that is, the presence of headache and scalp discomfort assessed by visual analogue scale (VAS, 0–10, 0: none, 5: medium, 10: extremely).

Results

Time-domain signals were presented as butterfly plots as well as voltage distribution across the scalp in Figure 2. Single-pulse TMS over the left DLPFC resulted in a series of negative and positive peaks including N45, P60, N120, and P200, in line with previous TMS-EEG studies assessed in the prefrontal cortex (Hill et al. 2017; Chung, Rogasch, Hoy, and Fitzgerald 2018; Chung, Rogasch, Hoy, Sullivan, et al. 2018; Che et al. 2019). Each peak showed a distinct pattern in scalp topography, indicating the spreading of voltage distribution across time.

Effects of rTMS on Pain Experience

The ANOVA revealed a main effect of time on cold pain threshold ($F_{1,33} = 4.492$, $P = 0.042$, partial $\eta^2 = 0.12$), with post hoc tests suggesting that both DLPFC and sham stimulations increased the pain threshold from pre- to poststimulation ($P_{Bonf} = 0.037$, $Mean_{Pre} = 6.682$, $Mean_{Post} = 7.316$) (Fig. 1c).

Plastic Effects of rTMS on TEPs

Grand average TEP waveforms are shown in Figure 3a,b. Cluster-based permutation tests revealed two significant clusters in N120 in DLPFC stimulation. The first cluster was a smaller N120 peak (i.e., positive) surrounding the following electrodes: F4, FC6, T8, FC2, C4, ($P_{corrected} = 0.008$). The other cluster was identified as a larger N120 peak (i.e., negative) surrounding the left electrodes: CP5, P3, P7, and O1, ($P_{corrected} = 0.014$) (Fig. 3c). Moreover, these two clusters demonstrated a strong negative correlation ($r = -0.853$, $P < 0.001$), indicating potential coherence between these two clusters (Fig. 3e).

Additionally, changes in the N120 amplitude were positively associated with increases in the pain threshold only in DLPFC stimulation ($r = 0.373$, $P = 0.030$) but not in the sham stimulation (Fig. 3f).

No other significant cluster was observed in other times of interest ($P_s > 0.05$). The sham stimulation revealed no significant changes in TEP ($P_s > 0.05$).

Source Localization

Source analysis identified increased activity in the right frontal cortices (Brodmann area [BA] 46 and Montreal Neurological Institute [MNI] coordinates: $X = 50$, $Y = 40$, $Z = 20$, $t = 0.257$, $P < 0.05$) as well as decreased source activity in the left insular cortices (Brodmann area [BA] 13 and Montreal Neurological Institute [MNI] coordinates: $X = -46$, $Y = 10$, $Z = 6$, $t = -0.202$, $P < 0.05$) (Fig. 3d).

Effects of rTMS on EEG Connectivity

NBS revealed a significant increase in gamma band coherence following DLPFC stimulation ($T = 2.95$, $P < 0.025$) (Fig. 4a), mainly between the prefrontal and somatosensory cortices (C3-Fz, F3-FC6) (Fig. 4b). No other significant clusters were observed in other frequency bands or times of interest by DLPFC stimulation ($P_s > 0.05$). No significant clusters were observed in the sham stimulation ($P_s > 0.05$).

Supplementary Results

In total, eight participants reported mild scalp discomfort in DLPFC stimulation ($Mean_{DLPFC} = 3.875$) and two in the sham condition ($Mean_{Sham} = 2.5$). Six participants reported mild headache in DLPFC stimulation ($Mean_{DLPFC} = 3.5$) and none in the sham condition. All these side effects disappeared by the end of the session.

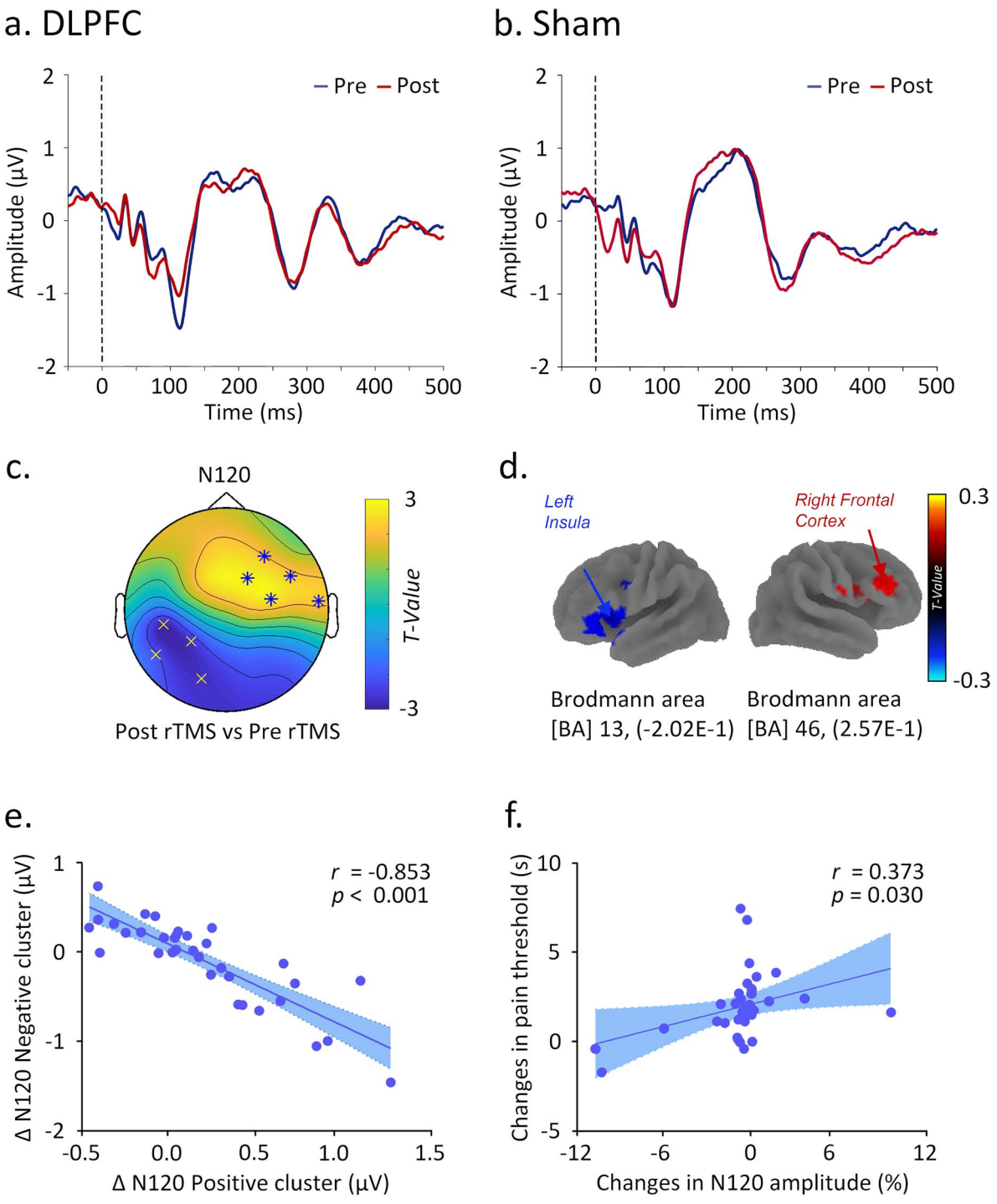

Figure 3. TEP results of rTMS. Grand average TEP waveforms from the electrode Fz is presented for illustration purposes in (*a*) DLPFC and (*b*) sham condition. (*c*) Indicates the two significant clusters in N120 following the DLPFC stimulation (right cortices: F4, FC6, T8, FC2, C4, $P_{corrected} = 0.008$, left cortices: CP5, P3, P7, O1, $P_{corrected} = 0.014$). (*d*) Source localization of N120 TEPs in the time window of 90–130 ms, results were located at the left insular and right prefrontal cortices, multiple comparison corrected at $P < 0.05$. (*e*) Illustrates the negative correlation between the two significant clusters of N120 in the DLPFC stimulation ($r = -0.853$, $P < 0.001$). (*f*) Illustrates the positive correlation between N120 changes and changes in pain thresholds ($r = 0.373$, $P = 0.030$). Error bar represents 95% confidence interval. *X* indicates $P < 0.05$, * indicates $P < 0.01$.

Discussion

Using concurrent TMS-EEG, the current study was designed to investigate the neuroplastic mechanisms of DLPFC analgesia. We provided novel evidence that DLPFC analgesia was associated with smaller N120 amplitude in the contralateral prefrontal cortex and larger N120 peak in the ipsilateral insular cortex. Further analysis revealed a strong negative correlation between N120 changes of these two regions. Changes in N120 amplitude were positively associated with increases in

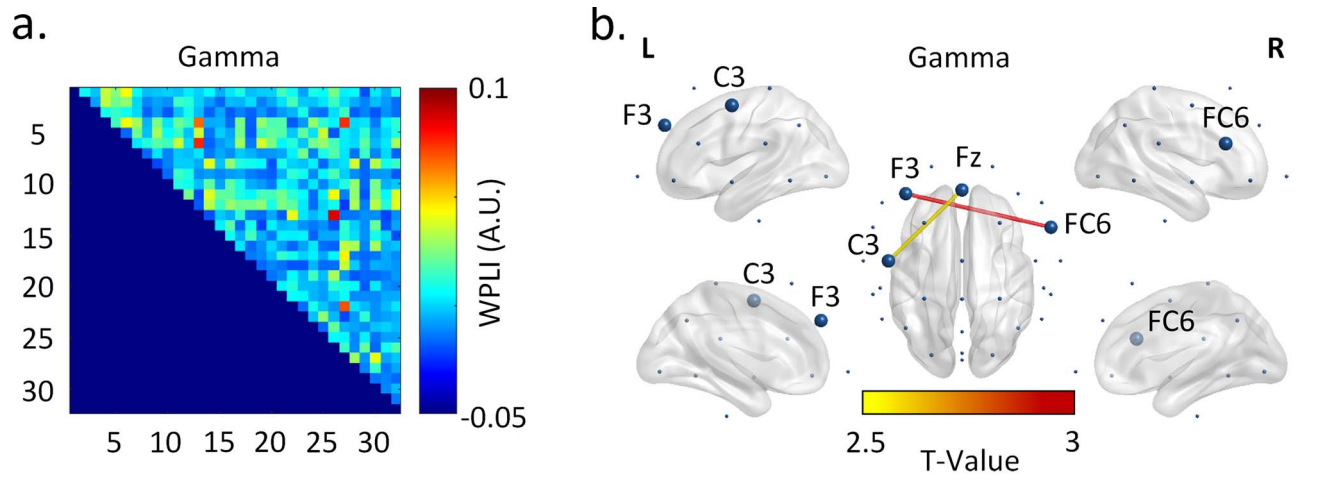

Figure 4. EEG connectivity and results. (*a*) A channel-by-channel correlation matrix for illustration purposes. (*b*) The DLPFC stimulation increased gamma band coherence between the prefrontal and sensorimotor cortices. Large dots highlight the significant electrodes, and the color and thickness of the lines indicate the *t* statistics. A.U. denotes arbitrary unit.

the pain threshold in DLPFC stimulation only. In addition, our data demonstrated enhanced coherence between the prefrontal and somatosensory cortices oscillating in the gamma frequency following DLPFC-rTMS. Although the sham stimulation was associated with pain reduction to some extent, there were no changes in local neuroplasticity or network property.

The cold pain data indicated that both DLPFC and sham stimulations increased the pain threshold (Fig. 1*c*). Although there was no significant difference, the increase in pain threshold seemed to be larger in DLPFC stimulation ($\Delta = 0.80$) compared with the sham ($\Delta = 0.48$) stimulation. Further analysis indicated that the increase in pain thresholds was positively associated with N120 amplitude changes in DLPFC stimulation but not in the sham stimulation (Fig. 3*f*). These findings corroborate the argument that the DLPFC is an important target for pain management (Fierro et al. 2010; Martin et al. 2013; Taylor et al. 2013; Seminowicz et al. 2018). Moreover, this finding is in line with our latest meta-analysis, which found that high-frequency rTMS over the DLPFC significantly reduced provoked pain (Che, Cash, et al. 2021). In addition, the sham stimulation may also be able to reduce the pain experience to some extent. Our TMS-EEG data indicated that this effect is not associated with neuroplastic changes (discussed next). Potential impacts caused by pain anticipation and/or habituation were also carefully controlled by initially exposing the left hand into the cold water. It is possible that the increased pain threshold in the sham stimulation is associated with a placebo effect as demonstrated in previous studies (Borckardt et al. 2014; Conforto et al. 2014; Granato et al. 2019).

We provided novel evidence that DLPFC stimulation resulted in a smaller N120 peak (positive cluster) in the contralateral prefrontal cortices (Fig. 3*c*). This finding was supplemented by the source evidence of increased brain activity in the contralateral prefrontal regions (Fig. 3*d*). The N120 is considered to reflect $GABA_B$-mediated intracortical inhibition (Premoli, Castellanos, et al. 2014; Premoli, Rivolta, et al. 2014; Darmani et al. 2019). Moreover, N120 amplitude in the nonstimulated hemisphere was decreased by the administration of $GABA_A$ agonists and/or modulators, suggesting the suppression of signal propagation under the influence of drugs with positive modulation at the $GABA_A$ receptor (Premoli, Castellanos, et al. 2014; Premoli, Rivolta, et al. 2014; Darmani et al. 2019). In addition, local GABA concentrations were found to be associated with decreased connectivity across hemispheres, in which local GABA levels are suggested to inhibit the spread of TMS-evoked activities (Du, Rowland, Summerfelt, Choa, et al. 2018). Our finding of smaller N120 in the contralateral prefrontal regions may be a result of $GABA_A$-mediated inhibition in the stimulated site following DLPFC stimulation.

More interestingly, our data demonstrated a larger N120 peak primarily in the left parietal regions following DLPFC stimulation (Fig. 3*c*). Source data further indicated decreased insular activity associated with this TEP change. As described above, a more negative N120 peak may therefore indicate increased $GABA_B$-mediated intracortical inhibition (Premoli, Castellanos, et al. 2014) in the insular cortex following DLPFC stimulation. It is widely accepted that the insular cortex is an essential component of the pain matrix, which is closely associated with the affective/emotional aspect of pain (Ostrowsky et al. 2002;Kishima et al. 2007 ; Bushnell et al. 2013). More interestingly, neuroplastic changes in the left insular cortex fits nicely into the fact that the right hand was exposed to cold pain. These results together indicate that DLPFC-rTMS is able to increase intracortical inhibition in the insular cortex, which is directly involved in the processing and modulation of the pain experience. This adds to the literature on the mechanisms of DLPFC analgesia by presenting novel

neuroplastic changes in the insular cortex that can be modulated by DLPFC stimulation.

In addition, there was a strong negative correlation between N120 changes in the prefrontal and insular cortices following DLPFC stimulation (Fig. 3*e*). This interesting finding indicates that DLPFC stimulation could entrain the synchronization between the prefrontal and insular cortices. The current distribution following single pulses is also consistent with this finding, which demonstrated a negative distribution surrounding the prefrontal cortex as well as a positive current distribution in the parietal-occipital regions in the N120 time window (Fig. 2*b*). These findings are in line with previous data of our group (Che et al. 2019) and of others (Rogasch et al. 2014; Chung, Rogasch, Hoy, and Fitzgerald 2018). More importantly, an increased pain threshold was positively associated with the amplitude changes encompassing both the positive and negative cluster but not with the positive or negative cluster alone (Fig. 3*f*). This finding provides direct evidence to support the synchronization between the prefrontal and insular cortices that likely contributes to DLPFC analgesia.

In addition, our data demonstrated that DLPFC-rTMS increased gamma band coherence between the prefrontal and somatosensory regions (Fig. 4). Gamma oscillations are believed to reflect GABAergic interneuron inhibition (Whittington et al. 1995; Leung and Shen 2007; Oren et al. 2010). Moreover, long interval cortical inhibition (LICI), a paired-pulse TMS paradigm to index $GABA_B$–receptor-mediated inhibitory neurotransmission, was found to suppress prefrontal gamma oscillation (Farzan et al. 2009). Our findings of increased gamma band coherence may, therefore, indicate increased inhibition over the somatosensory cortices following DLPFC stimulation. It is interesting to note that an increased pain threshold was associated with neuroplastic changes in the prefrontal–insula dyad but not with the coupling changes between the prefrontal and somatosensory regions. The insular cortex is suggested to mainly encode pain emotions (Kishima et al. 2007; Bushnell et al. 2013) while the somatosensory cortex more likely responds to the sensory aspects of pain (Craig 1996; Boadas-Vaello et al. 2016). Our findings therefore indicate that participants in this study might rely on unpleasant feelings to report cold pain.

Our data extend previous studies on potential mechanisms of DLPFC analgesia. A line of evidence indicated that rTMS over the DLPFC may drive top-down pain modulation, with studies demonstrating increased brain activation in the prefrontal cortex and decreased activity along thalamus, midbrain, and medulla following DLPFC stimulation (Martin et al. 2013; Taylor et al. 2013). Our data demonstrated neuroplastic changes in the prefrontal cortex as well as enhanced synchronization between the prefrontal and somatosensory cortices. Our findings agree with the descending pain modulation in a way that DLPFC-rTMS is capable of activating inhibitory circuits involved in nociceptive transmission. In addition to descending pain modulation, there is an argument that DLPFC may modulate corticocortical pathways, such as the insular cortex and ACC, in the modulation of pain (Lorenz et al. 2003; Tracey and Mantyh 2007). Our data provide direct evidence in which the DLPFC is able to modulate the neuroplastic changes in the insular cortex as well as its association with the changes in pain experience.

It is worth noting that TEPs can be easily contaminated by auditory and somatosensory artifacts during concurrent registrations (Rogasch et al. 2014). Rocchi et al. (2021) have carefully investigated the influence of auditory and somatosensory components on TEPs by adding a series of sensory control conditions. They found N120 and P200 to be enhanced by auditory and somatosensory stimulation, particularly locating over a large area surrounding the central electrodes. Meanwhile, the genuine cortical responses to single pulse TMS were more lateralized and much smaller. More importantly, these artifacts could be suppressed by appropriate noise masking (Rocchi et al. 2021). By using noise masking, our data demonstrated lateralized N120 changes in contralateral prefrontal and ipsilateral parietal electrodes, locating away from the central electrodes that could be associated with sensory artifacts. Moreover, source data indicated N120 changes to be associated with brain activations in the prefrontal and insular cortices. In addition, we found a significant relationship between increased pain threshold and N120 changes, further supporting the N120 changes reported here to reflect genuine cortical responses to TMS.

There are some limitations in this study. We used a 32-channel montage for TMS-EEG recordings. Although a 32-channel montage can be used to measure TEPs (Hill et al. 2017; Casula et al. 2018; Freedberg et al. 2020), higher density electrode arrays (e.g., 64) are more often used that can provide better spatial resolution. Nonetheless, we provided source data to assist in the localization of TEP changes. Future studies may wish to build on our findings and to investigate the neuroplastic changes in DLPFC analgesia with higher spatial resolution. Although the N120 changes reported here may not be contaminated by sensory artifacts, it is recommended to add certain sensory control techniques in TMS-EEG coregistration to assist in the identification of potential artifacts (Rocchi et al. 2021). Pain threshold was evaluated in this study, which has been most often used to measure provoked pain in DLPFC-rTMS studies (for a review, see Che, Fitzgibbon, et al. 2021). DLPFC-rTMS has also demonstrated consistent analgesia across the measurements of pain threshold and pain ratings (for a reviewer see Che, Fitzgibbon, et al. 2021). Nonetheless, future studies may wish to evaluate neuroplastic changes associated with different aspects of pain, such as pain intensity. In the current study, the duration of cold pain was too short to collect enough trials for EEG or TEP. In addition, the Beam F3 method was used here, which is considered sufficient and efficient for the localization of the DLPFC (Beam et al. 2009). However, a navigation system would

be able to increase targeting accuracy and assist in the identification of disease relevant brain connections and networks mediating positive treatment outcomes (Cash et al. 2021). Moreover, it is interesting for future studies to replicate our findings in old adults and even in individuals suffering from chronic pain. It is worth noting that there is an inconsistency in the literature on the latency of the negative peak around 100 ms. Most of the studies tended to term it as N100 or N120 based on their own data in the time domain (Rogasch et al. 2014; Chung et al. 2017; Premoli et al. 2018). Our data demonstrated the N120 peak surrounding 118 ms (Fig. 2*a*). Future studies may wish to investigate the confounders associated with the differences in peak latencies, such as the amplifying systems and the triggering latencies.

Our findings may bear clinical significance for optimizing the analgesic efficacy of DLPFC-rTMS. Our data indicated that DLPFC stimulation modulates the insular cortex, which is involved in nociceptive transmission and pain emotion and can be activated during noxious somatosensory stimulation. This finding highlights a potential circuit for future studies to modulate with brain stimulation techniques and therefore enhance the analgesic efficacy in clinical settings. Furthermore, the modulation of somatosensory cortex by DLPFC-rTMS may help to predict the response to rTMS treatment as the response rate in chronic pain is close to moderate and far from being excellent at its best (see Lefaucheur et al. 2014 for response rate). Indeed, there is evidence to demonstrate the potential of prediction models in optimizing the efficacy of rTMS treatment (Bailey et al. 2018). In addition, our data indicate immediate neuroplastic changes following a single-session TMS intervention. This result highlights the potential of repetitive sessions in the management of pain experience as rTMS treatments tend to be underdosed in chronic pain studies compared to the treatments of depression (Che, Cash, et al. 2021).

In conclusion, the analgesic effects of DLPFC were associated with GABAergic neuroplastic changes in the prefrontal cortex and the insular cortex as demonstrated by concurrent TMS-EEG. DLPFC stimulation further demonstrated enhanced connectivity between the prefrontal cortex and the somatosensory cortex oscillating in the gamma frequency. Overall, we present novel evidence on local and distributed neuroplastic changes associated with DLPFC analgesia.

Supplementary Material

Supplementary material can be found at *Cerebral Cortex* online.

Funding

National Natural Science Foundation of China (4045F4112 0040); Provincial Advantage Discipline Project (20JYXK034); Key Medical Disciplines of Hangzhou.

Notes

Conflict of Interest: The authors declare no competing financial interests.

Data Availability

All the data and codes generating findings of this work are available upon the request from the corresponding author.

References

Bailey NW, Hoy KE, Rogasch NC, Thomson RH, McQueen S, Elliot D, Sullivan CM, Fulcher BD, Daskalakis ZJ, Fitzgerald PB. 2018. Responders to rTMS for depression show increased fronto-midline theta and theta connectivity compared to non-responders. *Brain Stimul*. 11:190–203.

Beam W, Borckardt JJ, Reeves ST, George MS. 2009. An efficient and accurate new method for locating the F3 position for prefrontal TMS applications. *Brain Stimul*. 2:50–54.

Belardinelli P, Konig F, Liang C, Premoli I, Desideri D, Muller-Dahlhaus F, Gordon PC, Zipser C, Zrenner C, Ziemann U. 2021. TMS-EEG signatures of glutamatergic neurotransmission in human cortex. *Sci Rep*. 11:8159.

Boadas-Vaello P, Castany S, Homs J, Alvarez-Perez B, Deulofeu M, Verdu E. 2016. Neuroplasticity of ascending and descending pathways after somatosensory system injury: reviewing knowledge to identify neuropathic pain therapeutic targets. *Spinal Cord*. 54: 330–340.

Borckardt JJ, Reeves ST, Kotlowski P, Abernathy JH, Field LC, Dong L, Frohman H, Moore H, Ryan K, Madan A, et al. 2014. Fast left prefrontal rTMS reduces post-gastric bypass surgery pain: findings from a large-scale, double-blind, sham-controlled clinical trial. *Brain Stimul*. 7:42–48.

Bushnell MC, Ceko M, Low LA. 2013. Cognitive and emotional control of pain and its disruption in chronic pain. *Nat Rev Neurosci*. 14: 502–511.

Cash RFH, Noda Y, Zomorrodi R, Radhu N, Farzan F, Rajji TK, Fitzgerald PB, Chen R, Daskalakis ZJ, Blumberger DM. 2017. Characterization of glutamatergic and GABAA-mediated neurotransmission in motor and dorsolateral prefrontal cortex using paired-pulse TMS-EEG. *Neuropsychopharmacology*. 42:502–511.

Cash RFH, Weigand A, Zalesky A, Siddiqi SH, Downar J, Fitzgerald PB, Fox MD. 2021. Using brain imaging to improve spatial targeting of transcranial magnetic stimulation for depression. *Biol Psychiatry*. 90:689–700.

Casula EP, Rocchi L, Hannah R, Rothwell JC. 2018. Effects of pulse width, waveform and current direction in the cortex: a combined cTMS-EEG study. *Brain Stimulation*. 11:1063–1070.

Che X, Cash R, Fitzgerald P, Fitzgibbon BM. 2018. The social regulation of pain: autonomic and neurophysiological changes associated with perceived threat. *J Pain*. 19:496–505.

Che X, Cash R, Chung SW, Bailey N, Fitzgerald PB, Fitzgibbon BM. 2019. The dorsomedial prefrontal cortex as a flexible hub mediating behavioral as well as local and distributed neural effects of social support context on pain: a theta burst stimulation and TMS-EEG study. *NeuroImage*. 201:116053.

Che X, Cash RFH, Luo X, Luo H, Lu X, Xu F, Zang YF, Fitzgerald PB, Fitzgibbon BM. 2021. High-frequency rTMS over the dorsolateral prefrontal cortex on chronic and provoked pain: a systematic review and meta-analysis. *Brain Stimul*. 14:1135–1146.

Che X, Fitzgibbon BM, Ye Y, Wang J, Luo H, Fitzgerald PB, Cash RFH. 2021. Characterising the optimal pulse number and frequency for inducing analgesic effects with motor cortex rTMS. *Brain Stimul*. 14:1081–1083.

Chung SW, Lewis BP, Rogasch NC, Saeki T, Thomson RH, Hoy KE, Bailey NW, Fitzgerald PB. 2017. Demonstration of short-term plasticity in the dorsolateral prefrontal cortex with theta burst stimulation: a TMS-EEG study. *Clin Neurophysiol*. 128:1117–1126.

Chung SW, Rogasch NC, Hoy KE, Fitzgerald PB. 2018. The effect of single and repeated prefrontal intermittent theta burst stimulation on cortical reactivity and working memory. *Brain Stimul*. 11: 566–574.

Chung SW, Rogasch NC, Hoy KE, Sullivan CM, Cash RFH, Fitzgerald PB. 2018. Impact of different intensities of intermittent theta burst stimulation on the cortical properties during TMS-EEG and working memory performance. *Hum Brain Mapp*. 39: 783–802.

Conforto AB, Amaro E Jr, Goncalves AL, Mercante JP, Guendler VZ, Ferreira JR, Kirschner CC, Peres MF. 2014. Randomized, proof-of-principle clinical trial of active transcranial magnetic stimulation in chronic migraine. *Cephalalgia*. 34:464–472.

Craig AD. 1996. Chapter 13: an ascending general homeostatic afferent pathway originating in lamina I. *Prog Brain Res*. 107:225–242.

Darmani G, Bergmann TO, Zipser C, Baur D, Muller-Dahlhaus F, Ziemann U. 2019. Effects of antiepileptic drugs on cortical excitability in humans: a TMS-EMG and TMS-EEG study. *Hum Brain Mapp*. 40:1276–1289.

de Andrade DC, Mhalla A, Adam F, Texeira MJ, Bouhassira D. 2011. Neuropharmacological basis of rTMS-induced analgesia: the role of endogenous opioids. *Pain*. 152:320–326.

de Andrade DC, Mhalla A, Adam F, Texeira MJ, Bouhassira D. 2014. Repetitive transcranial magnetic stimulation induced analgesia depends on N-methyl-D-aspartate glutamate receptors. *Pain*. 155: 598–605.

De Martino E, Fernandes AM, Galhardoni R, De Oliveira SC, Ciampi De Andrade D, Graven-Nielsen T. 2019. Sessions of prolonged continuous theta burst stimulation or high-frequency 10 Hz stimulation to left dorsolateral prefrontal cortex for 3 days decreased pain sensitivity by modulation of the efficacy of conditioned pain modulation. *J Pain*. 20:1459–1469.

Delorme A, Makeig S. 2004. EEGLAB: an open source toolbox for analysis of single-trial EEG dynamics including independent component analysis. *J Neurosci Methods*. 134:9–21.

Du X, Rowland LM, Summerfelt A, Choa FS, Wittenberg GF, Wisner K, Wijtenburg A, Chiappelli J, Kochunov P, Hong LE. 2018. Cerebellar-stimulation evoked prefrontal electrical synchrony is modulated by GABA. *Cerebellum*. 17:550–563.

Du X, Rowland LM, Summerfelt A, Wijtenburg A, Chiappelli J, Wisner K, Kochunov P, Choa FS, Hong LE. 2018. TMS evoked N100 reflects local GABA and glutamate balance. *Brain Stimul*. 11:1071–1079.

Farzan F, Barr MS, Wong W, Chen R, Fitzgerald PB, Daskalakis ZJ. 2009. Suppression of gamma-oscillations in the dorsolateral prefrontal cortex following long interval cortical inhibition: a TMS-EEG study. *Neuropsychopharmacology*. 34:1543–1551.

Fierro B, De Tommaso M, Giglia F, Giglia G, Palermo A, Brighina F. 2010. Repetitive transcranial magnetic stimulation (rTMS) of the dorsolateral prefrontal cortex (DLPFC) during capsaicin-induced pain: modulatory effects on motor cortex excitability. *Exp Brain Res*. 203:31–38.

Fitzgerald PB, Daskalakis ZJ, Hoy K, Farzan F, Upton DJ, Cooper NR, Maller JJ. 2008. Cortical inhibition in motor and non-motor regions: a combined TMS-EEG study. *Clin EEG Neurosci*. 39: 112–117.

Freedberg M, Reeves JA, Hussain SJ, Zaghloul KA, Wassermann EM. 2020. Identifying site- and stimulation-specific TMSevoked EEG potentials using a quantitative cosine similarity metric. *PLoS One*. 15(1):e0216185.

Granato A, Fantini J, Monti F, Furlanis G, Musho Ilbeh S, Semenic M, Manganotti P. 2019. Dramatic placebo effect of high frequency repetitive TMS in treatment of chronic migraine and medication overuse headache. *J Clin Neurosci*. 60:96–100.

Hill AT, Rogasch NC, Fitzgerald PB, Hoy KE. 2017. Effects of prefrontal bipolar and high-definition transcranial direct current stimulation on cortical reactivity and working memory in healthy adults. *NeuroImage*. 152:142–157.

Hosomi K, Sugiyama K, Nakamura Y, Shimokawa T, Oshino S, Goto Y, Mano T, Shimizu T, Yanagisawa T, Saitoh Y, et al. 2020. A randomized controlled trial of 5 daily sessions and continuous trial of 4 weekly sessions of repetitive transcranial magnetic stimulation for neuropathic pain. *Pain*. 161:351–360.

Kishima H, Saitoh Y, Osaki Y, Nishimura H, Kato A, Hatazawa J, Yoshimine T. 2007. Motor cortex stimulation in patients with deafferentation pain: activation of the posterior insula and thalamus. *J Neurosurg*. 107:43–48.

Lefaucheur J, Drouot X, Menard-Lefaucheur I, Keravel Y, Nguyen J. 2006. Motor cortex rTMS restores defective intracortical inhibition in chronic neuropathic pain. *Neurology*. 67:1568–1574.

Lefaucheur JP, Drouot X, Menard-Lefaucheur I, Keravel Y, Nguyen JP. 2008. Motor cortex rTMS in chronic neuropathic pain: pain relief is associated with thermal sensory perception improvement. *J Neurol Neurosurg Psychiatry*. 79:1044–1049.

Lefaucheur JP, Andre-Obadia N, Antal A, Ayache SS, Baeken C, Benninger DH, Cantello RM, Cincotta M, de Carvalho M, De Ridder D, et al. 2014. Evidence-based guidelines on the therapeutic use of repetitive transcranial magnetic stimulation (rTMS). *Clin Neurophysiol*. 125:2150–2206.

Leung LS, Shen B. 2007. GABAB receptor blockade enhances theta and gamma rhythms in the hippocampus of behaving rats. *Hippocampus*. 17:281–291.

Leung A, Metzger-Smith V, He Y, Cordero J, Ehlert B, Song D, Lin L, Shahrokh G, Tsai A, Vaninetti M, et al. 2018. Left dorsolateral prefrontal cortex rTMS in alleviating MTBI related headaches and depressive symptoms. *Neuromodulation*. 21:390–401.

Lorenz J, Minoshima S, Casey K. 2003. Keeping pain out of mind: the role of the dorsolateral prefrontal cortex in pain modulation. *Brain*. 126:1079–1091.

Lowery D, Fillingim RB, Wright RA. 2003. Sex differences and incentive effects on perceptual and cardiovascular responses to cold pressor pain. *Psychosom Med*. 65:284–291.

Maris E, Oostenveld R. 2007. Nonparametric statistical testing of EEG- and MEG-data. *J Neurosci Methods*. 164:177–190.

Martin L, Borckardt JJ, Reeves ST, Frohman H, Beam W, Nahas Z, Johnson K, Younger J, Madan A, Patterson D. 2013. A pilot functional MRI study of the effects of prefrontal rTMS on pain perception. *Pain Med*. 14:999–1009.

Mitchell LA, MacDonald RA, Brodie EE. 2004. Temperature and the cold pressor test. *J Pain*. 5:233–237.

Mulert C, Jäger L, Schmitt R, Bussfeld P, Pogarell O, Möller H-J, Juckel G, Hegerl U. 2004. Integration of fMRI and simultaneous EEG: towards a comprehensive understanding of localization and time-course of brain activity in target detection. *NeuroImage*. 22: 83–94.

Nahmias F, Debes C, de Andrade DC, Mhalla A, Bouhassira D. 2009. Diffuse analgesic effects of unilateral repetitive transcranial magnetic stimulation (rTMS) in healthy volunteers. *Pain*. 147: 224–232.

Oostenveld R, Fries P, Maris E, Schoffelen J-M. 2011. FieldTrip: open source software for advanced analysis of MEG, EEG, and invasive electrophysiological data. *Comput Intell Neurosci*. 2011:156869.

Oren I, Hajos N, Paulsen O. 2010. Identification of the current generator underlying cholinergically induced gamma frequency field potential oscillations in the hippocampal CA3 region. *J Physiol*. 588:785–797.

Ostrowsky K, Magnin M, Ryvlin P, Isnard J, Guenot M, Mauguiere F. 2002. Representation of pain and somatic sensation in the human insula: a study of responses to direct electrical cortical stimulation. *Cereb Cortex*. 12:376–385.

Ozdemir RA, Boucher P, Fried PJ, Momi D, Jannati A, Pascual-Leone A, Santarnecchi E, Shafi MM. 2021. Reproducibility of cortical response modulation induced by intermittent and continuous theta-burst stimulation of the human motor cortex. *Brain Stimul*. 14:949–964.

Ozdemir RA, Tadayon E, Boucher P, Sun H, Momi D, Ganglberger W, Westover MB, Pascual-Leone A, Santarnecchi E, Shafi MM. 2021. Cortical responses to noninvasive perturbations enable individual brain fingerprinting. *Brain Stimul*. 14:391–403.

Pascual-Leone A, Tormos JM, Keenan J, Tarazona F, Cañete C, Catalá MD. 1998. Study and modulation of human cortical excitability with transcranial magnetic stimulation. *J Clin Neurophysiol*. 15: 333–343.

Pascual-Marqui RD. 2002. Standardized low-resolution brain electromagnetic tomography (sLORETA): technical details. *Methods Find Exp Clin Pharmacol*. 24:5–12.

Passard A, Attal N, Benadhira R, Brasseur L, Saba G, Sichere P, Perrot S, Januel D, Bouhassira D. 2007. Effects of unilateral repetitive transcranial magnetic stimulation of the motor cortex on chronic widespread pain in fibromyalgia. *Brain*. 130:2661–2670.

Pisoni A, Romero Lauro LJ, Vergallito A, Maddaluno O, Bolognini N. 2018. Cortical dynamics underpinning the self-other distinction of touch: a TMS-EEG study. *NeuroImage*. 178:475–484.

Pizzagalli DA, Greischar LL, Davidson RJ. 2003. Spatio-temporal dynamics of brain mechanisms in aversive classical conditioning: high-density event-related potential and brain electrical tomography analyses. *Neuropsychologia*. 41:184–189.

Premoli I, Castellanos N, Rivolta D, Belardinelli P, Bajo R, Zipser C, Espenhahn S, Heidegger T, Muller-Dahlhaus F, Ziemann U. 2014. TMS-EEG signatures of GABAergic neurotransmission in the human cortex. *J Neurosci*. 34:5603–5612.

Premoli I, Rivolta D, Espenhahn S, Castellanos N, Belardinelli P, Ziemann U, Muller-Dahlhaus F. 2014. Characterization of GABAB-receptor mediated neurotransmission in the human cortex by paired-pulse TMS-EEG. *NeuroImage*. 103:152–162.

Premoli I, Bergmann TO, Fecchio M, Rosanova M, Biondi A, Belardinelli P, Ziemann U. 2017. The impact of GABAergic drugs on TMS-induced brain oscillations in human motor cortex. *NeuroImage*. 163:1–12.

Premoli I, Kiraly J, Muller-Dahlhaus F, Zipser CM, Rossini P, Zrenner C, Ziemann U, Belardinelli P. 2018. Short-interval and long-interval intracortical inhibition of TMS-evoked EEG potentials. *Brain Stimul*. 11:818–827.

Rainville P, Feine JS, Bushnell MC, Duncan GH. 1992. A psychophysical comparison of sensory and affective responses to four modalities of experimental pain. *Somatosens Mot Res*. 9:265–277.

Rocchi L, Ibanez J, Benussi A, Hannah R, Rawji V, Casula E, Rothwell J. 2018. Variability and predictors of response to continuous theta burst stimulation: a TMS-EEG study. *Front Neurosci*. 12:400.

Rocchi L, Di Santo A, Brown K, Ibanez J, Casula E, Rawji V, Di Lazzaro V, Koch G, Rothwell J. 2021. Disentangling EEG responses to TMS due to cortical and peripheral activations. *Brain Stimul*. 14: 4–18.

Rogasch NC, Thomson RH, Daskalakis ZJ, Fitzgerald PB. 2013. Short-latency artifacts associated with concurrent TMS-EEG. *Brain Stimul*. 6:868–876.

Rogasch NC, Thomson RH, Farzan F, Fitzgibbon BM, Bailey NW, Hernandez-Pavon JC, Daskalakis ZJ, Fitzgerald PB. 2014. Removing artefacts from TMS-EEG recordings using independent component analysis: importance for assessing prefrontal and motor cortex network properties. *NeuroImage*. 101:425–439.

Rogasch NC, Sullivan C, Thomson RH, Rose NS, Bailey NW, Fitzgerald PB, Farzan F, Hernandez-Pavon JC. 2017. Analysing concurrent transcranial magnetic stimulation and electroencephalographic data: a review and introduction to the open-source TESA software. *NeuroImage*. 147:934–951.

Rossi S, Hallett M, Rossini PM, Pascual-Leone A. 2011. Screening questionnaire before TMS: an update. *Clin Neurophysiol*. 122:1686.

Santarcangelo EL, Paoletti G, Chiavacci I, Palombo C, Carli G, Varanini M. 2013. Cognitive modulation of psychophysical, respiratory and autonomic responses to cold pressor test. *PLoS One*. 8:e75023.

Seminowicz DA, de Martino E, Schabrun SM, Graven-Nielsen T. 2018. Left dorsolateral prefrontal cortex repetitive transcranial magnetic stimulation reduces the development of long-term muscle pain. *Pain*. 159:2486–2492.

Sheehan D, Lecrubier Y. 2001. *Mini screen 5.0. 0/English version/DSM-IV July/1/06*. Florida: University of South Florida-TAMPA, USA.

Short BE, Borckardt JJ, Anderson BS, Frohman H, Beam W, Reeves ST, George MS. 2011. Ten sessions of adjunctive left prefrontal rTMS significantly reduces fibromyalgia pain: a randomized, controlled pilot study. *Pain*. 152:2477–2484.

Summers J, Johnson S, Pridmore S, Oberoi G. 2004. Changes to cold detection and pain thresholds following low and high frequency transcranial magnetic stimulation of the motor cortex. *Neurosci Lett*. 368:197–200.

Taylor JJ, Borckardt JJ, Canterberry M, Li X, Hanlon CA, Brown TR, George MS. 2013. Naloxone-reversible modulation of pain circuitry by left prefrontal rTMS. *Neuropsychopharmacology*. 38: 1189–1197.

Tracey I, Mantyh PW. 2007. The cerebral signature for pain perception and its modulation. *Neuron*. 55:377–391.

Vase L, Robinson ME, Verne GN, Price DD. 2005. Increased placebo analgesia over time in irritable bowel syndrome (IBS) patients is associated with desire and expectation but not endogenous opioid mechanisms. *Pain*. 115:338–347.

Vinck M, Oostenveld R, Van Wingerden M, Battaglia F, Pennartz CM. 2011. An improved index of phase-synchronization for electrophysiological data in the presence of volume-conduction, noise and sample-size bias. *NeuroImage*. 55:1548–1565.

Wager TD, Rilling JK, Smith EE, Sokolik A, Casey KL, Davidson RJ, Kosslyn SM, Rose RM, Cohen JD. 2004. Placebo-induced changes in FMRI in the anticipation and experience of pain. *Science*. 303: 1162–1167.

Whittington MA, Traub RD, Jefferys JG. 1995. Synchronized oscillations in interneuron networks driven by metabotropic glutamate receptor activation. *Nature*. 373:612–615.

Wilcox RR. 2011. *Introduction to robust estimation and hypothesis testing*. San Diego, (CA): Academic Press.

Xia M, Wang J, He Y. 2013. BrainNet viewer: a network visualization tool for human brain connectomics. *PLoS One*. 8:e68910.

Zalesky A, Fornito A, Bullmore ET. 2010. Network-based statistic: identifying differences in brain networks. *NeuroImage*. 53: 1197–1207.